inter noise
2013 | INNSBRUCK | AUSTRIA
15.-18. SEPTEMBER 2013
NOISE CONTROL FOR QUALITY OF LIFE

Use of hand held array for NVH measurement in the automotive industry

Svend Gade[1], Jesper Gomes[2], and Jørgen Hald[3]

[1,2,3] Brüel & Kjær Sound & Vibration Measurement A/S,

Skodsborgvej 307,2850 Nærum, Denmark

ABSTRACT

The use of single layer and double layer microphone arrays, both hand held as well as robot operated, has been greatly extended within the last decade. This paper summarizes how a small double layer array with typically 128 microphones can be used for interior cabin measurements for mapping various acoustical properties. There are four major applications. The first one is general patch holography (or conformal mapping) of basic acoustical quantities like sound pressure, particle velocity and sound intensity. Optionally sound quality (SQ) metrics for describing human annoyance like loudness, sharpness, fluctuation strength and roughness etc. can also be mapped. Other applications are in-situ absorption measurement - for example inside a car cabin, intensity component analysis (e.g. incident, reflected, scattered, net intensity etc. can be separated) and finally sound pressure contribution from various panels inside cabins to an operators/drivers position. Some measurements are done in operational condition and some are reference laboratory measurement of typical frequency response functions.

Keywords: Holography, Array, NVH

1. INTRODUCTION

Traditional Nearfield Acoustic Holography, NAH was introduced in the mid 1980'ies [1-2]. NAH allows you to obtain a complete model of the sound field in the vicinity of a sound source, i.e. all sound field quantities (sound pressure, particle velocity, active and reactive intensity) can be calculated at any location based of pressure measurements on a planar surface in front of the sound source. In particular, the sound field can be mapped closer to the source than the measurement plane, which can provide very high spatial resolution of the source distribution. NAH was typically implemented in the spatial frequency domain using a two dimensional (2D) Spatial Fourier Transform. Detailed information about how to implement the calculations is found in Ref. [3]. One of the drawbacks of the original formulation was that the measurement area should adequately cover the full source plus some "additional" more, so the basic hypothesis that practically all energy of the sound field radiated into the half-space passes through the measurement window was fulfilled. The upper frequency limit is given by that microphone spacing must be less than half wavelength in order to avoid spatial aliasing.

1 Svend.Gade@bksv.com
2 Jesper.Gomes@bksv.com
3 Jorgen.Hald@bksv.com

Practical measurements were performed using a sub-array and scan techniques. Reference transducers are needed in order to link the scan measurement together [4-5].

Statistically Optimized Nearfield Acoustic Holography, SONAH became a new formulation of NAH performing the plane-to-plane transformation directly in the spatial domain avoiding the use of spatial DFT thus avoiding/eliminating windowing and leakage errors associated with FFT/DFT calculations. SONAH opens up for the use of holography measurements with an array that is much smaller than the source, e.g. small hand-held arrays and still keeping errors at an acceptable level [6-7]. SONAH also opens up for introduction of irregular array geometries that can be used for both holography measurements (low to medium frequencies) and beamforming (medium to high frequencies) thus covering the full frequency range [8].

The first application of a small array was patch holography, where you just take measurement where it is relevant (for example around a door seal for sound leakage detection) rather than measuring around the whole vehicle. Today the use of a small array has been extended to several applications such as in-situ absorption measurement, intensity component analysis (e.g. incident, reflected, scattered, net intensity etc.) and panel contribution. Also a more precise core holography algorithm - similar to SONAH - Equivalent Source Method, ESM for measuring on curved surfaces has been developed recently [9-10], see figure 1. This paper will give an overview of the four applications, as well as the new ESM algorithm.

2. EQUIVALENT SOURCE METHOD, ESM

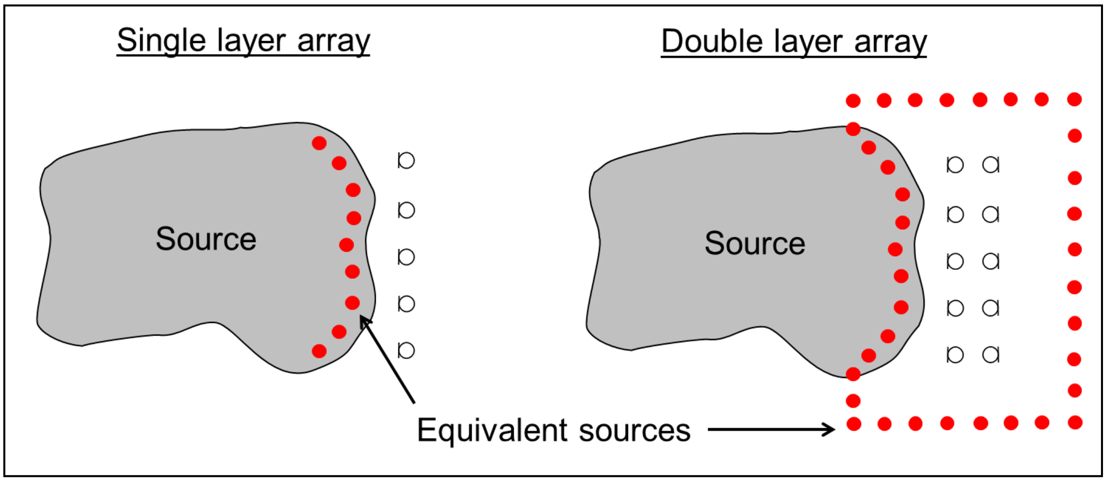

Figure 1a – ESM modeling using Single Layer Array, Figure 1b – ESM modeling using Double Layer Array

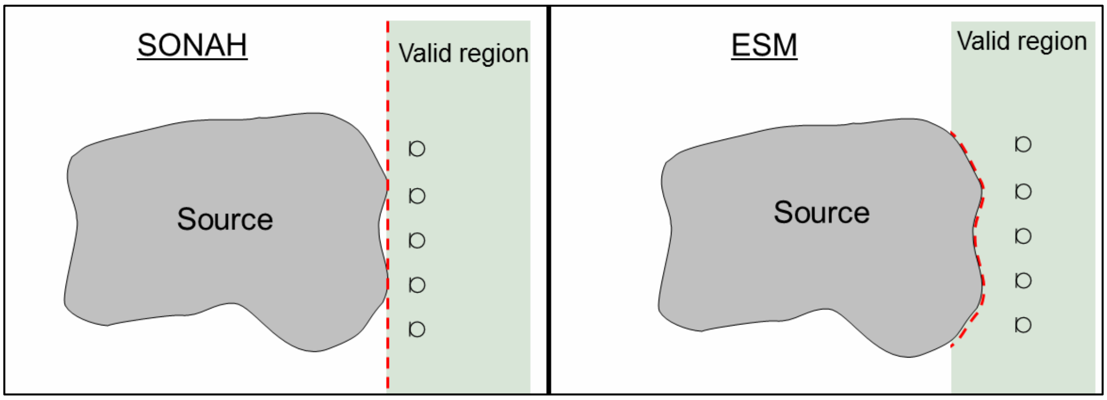

Figure 2a – Valid region of SONAH algorithm, Figure 2b – Valid region of ESM algorithm

Using ESM the acoustic field is predicted directly by a mesh set of weighted equivalent monopole sources located inside the vibrating body so the method is suitable for arbitrary source shapes, see figure 1a. Here the requirement of having a model that can represent all contributions to the sound field in the test region is not fulfilled, but because of the short distance between the measurement area and reconstruction area a good approximation for the local patch can be expected.

Furthermore if the mesh is arranged, so that it surrounds a two-layer microphone array, and with a part of the mesh surface coinciding with the patch of interest then the requirement of having a model that can represent all contributions to the sound field in the test region is fulfilled for a local sound field modeling, see figure 1b. Global sound field modeling is then obtained by a series of patch measurement. In addition, using an array with two layers, sources are allowed behind the array.

The major difference between SONAH and ESM from an application point of view is that ESM handles arbitrary shaped sources and curved surfaces better than SONAH, see figure 2. SONAH uses a sound field model in terms of plane propagating and evanescent waves, whereas EMS uses a source model. So where ESM relies on the definition of a sufficient set of monopole sources this is not the case for SONAH.

3. INSTRUMENTATION

The measurement system is described in details in Ref. [11]. The sound field measuring part consist of a 128 ch. hand held microphone array (figure 3a), a 132 ch. LAN-XI front end (figure 3b), a positioning system integrated into the array frame and a pc with dedicated software.

The array has 8x8 microphones mounted in 2 layers, resulting in a total of 128 microphones. The microphones are spaced 25 mm (various distances 25-50 mm are available) apart in both directions and with a spacing of 31 mm between the two layers. This results in an upper frequency limit for the array of 5 kHz (spatial sampling limit). Due to corrections for phase response (stored in Transducer Electronic Data Sheet, TEDS information) the array performs to frequencies very well below 200 Hz. In general TEDS corrections will improve the available dynamic range over a broad frequency range [13-14]. The array is connected to the front end via a single cable as shown in figure 3b.

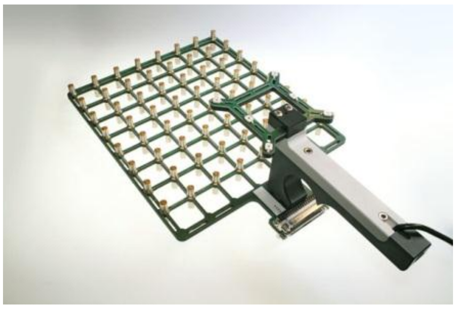

Figure 3a – Double layer array with 8x8x2 microphones

Figure 3b – 132 ch. Front end with single cable connection to the array

A 3D Creator system consisting of an optical sensor unit, a digitizer control unit, a wireless hand-held probe, and a wired Dynamic Reference Frame enables precise three-dimensional measurement of array position in real-time as well as capturing of the surface geometry of the device under test.

4. APPLICATIONS OF HAND HELD ARRAY

Today four major applications of a small hand held array exist: Patch holography, absorption measurements, intensity component analysis and panel contribution.

4.1 Patch Holography / Conformal Mapping

This is the fundamental application of a hand held microphone array. First a geometry surface model can be created by the positioning system or imported from a CAD model. The actual measurements are done with the small, double layer array, DLA (for interior noise measurements, diffuse sound fields) or single layer array, SLA (for exterior noise measurement, semi-anechoic sound fields) mounted on a handle with a built-in 3D position measurement system, see figure 3a. The system continuously determines the positions of the array microphones relative to some user-defined coordinate system. To map the sound field on a surface larger than the array, patch measurements are made with the array in neighboring (preferably overlapping) positions over the surface. In each array patch position, acoustic and position data belonging together is recorded. Patch positions already visited/measured are displayed in a 3D view along with the real-time updated current position of the array. Also shown in the 3D view is a surface model of the test object. In this way, the user is guided in covering the surface area with sufficient array patch positions in order to obtain a reliable surface mapping result. To minimize the errors in the patch holography calculations, a very small measurement distance is recommended, typically equal to half of the microphone grid spacing. If this is not possible, then patches with significant overlap should be used, avoiding the need to perform calculations near the boundaries of the array areas. The procedure is visualized in figure 4 using a simple loudspeaker (ghetto blaster) example. Figure 4a shows the individual six measurement patches (with no or little overlap) while figure 4b shows the sound intensity results of the patch holography / conformal mapping. Typical sound field quantities like sound pressure, particle velocity and sound intensity can be mapped. Optionally sound quality (SQ) metrics for describing human annoyance like loudness, sharpness, fluctuation strength and roughness etc. can also be mapped.

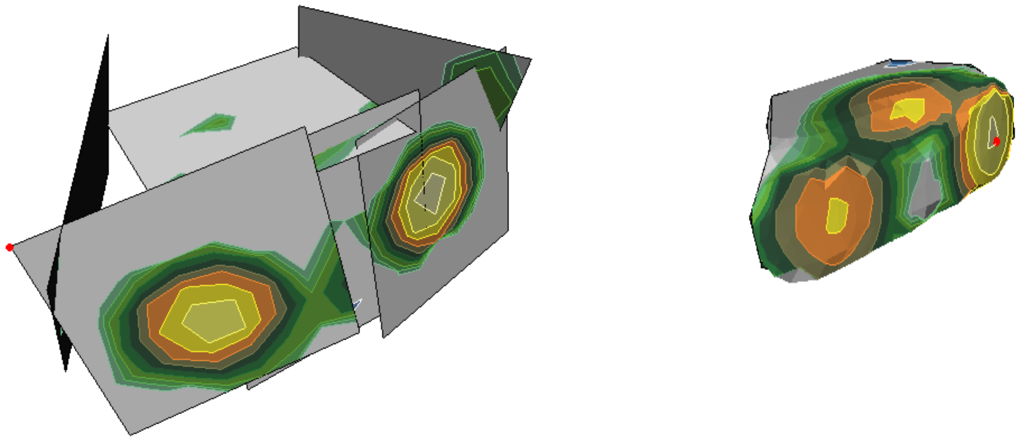

Figure 4a – Six measurement patches, Figure 4b – Patch Holography / Conformal Mapping results

4.2 In situ absorption measurements

The double layer array in combination with holography calculations yields the 3 intensity components, the net/total intensity, positive (from front direction) and negative (from rear direction) intensity.

$$I_{tot}(I_{net}) = I_{front} + I_{rear} = I_{rad} + I_{abs} \quad (1)$$

When measuring for the estimation of surface absorption, a number of loudspeakers are distributed in the cabin interior and driven by uncorrelated noise sources, to create a distributed and (close-to) diffuse excitation field. The net intensity is also the sum of the radiated and absorbed intensity, thus in this simple case ($I_{rad} = 0$) the absorption coefficient, α can be calculated from

$$I_{tot} = I_{abs} = \alpha I_{rear} \quad (2)$$

I.e. α can be calculated when I_{tot} and I_{rear} are known. See Refs. [11,15] for a more detailed discussion.

To illustrate the use of the proposed techniques in an automotive application, measurements were made with the DLA system in the cabin of a Volvo S60 passenger car to determine the in-situ absorption coefficient of selected surfaces in the cabin. Firstly, the cabin surfaces to be investigated were digitized using the 3D position measurement system and dedicated digitizing software. Next, array measurements were made with the DLA covering the surfaces patch by patch. Four loudspeakers were distributed in the cabin and driven by uncorrelated white noise to provide the acoustic excitation needed for the estimation of the absorption coefficient [11].

Figure 5 shows a 3D contour plot of the estimated absorption coefficient on the cabin surfaces for the 200 Hz 1/3 octave band. The absorption coefficient was estimated by first doing 1/3 octave band synthesis of the estimated total and incident/rear intensities, and then doing area averaging of these quantities over e.g. the seat or window surface before estimating the final absorption coefficient as the ratio between the two. The figure shows that in the 200 Hz frequency band the seat has quite a high absorption coefficient compared to the door, window and roof.

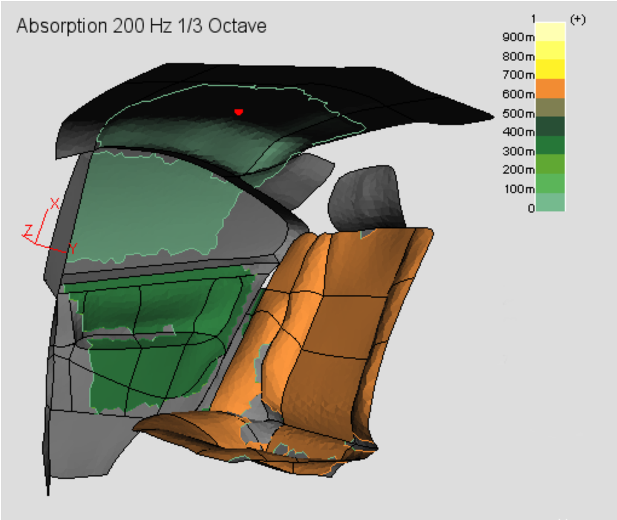

Figure 5 – A contour plot of the estimated absorption coefficient of seat, door, window and roof in a car cabin. Results shown for the 200 Hz 1/3-octave band are averaged over the respective areas.

4.3 Intensity component analysis

Consider the radiation of sound from a small surface segment in a cabin environment. Such a surface segment may radiate sound energy because of external forcing, causing the surface to vibrate, and it may absorb energy from an incident sound field because of finite surface acoustic impedance. When measuring the sound intensity over the surface segment with an intensity probe, only total intensity I_{tot} will be estimated. Holography can also separate into front and rear intensities, figure 6a and eq. (3).

$$(p_{total}, \boldsymbol{u}_{total}) = (p_{front}, \boldsymbol{u}_{front}) + (p_{rear}, \boldsymbol{u}_{rear}) \qquad (3)$$

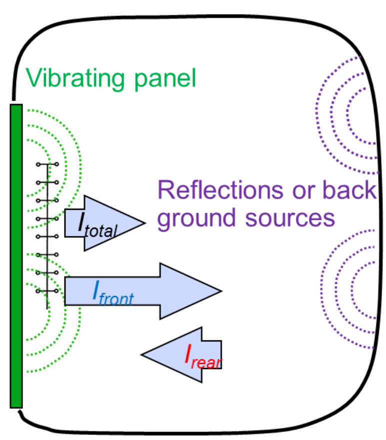

Figure 6a – Net intensity is a summation of positive and negative going intensities

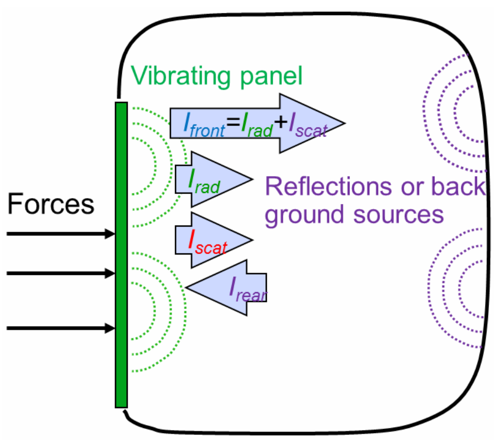

Figure 6b – Positive intensity is a summation of radiated and scattered intensities

By visualizing figures 6a & 6b we can further more set up a couple of additional equations relating the different intensity components, radiated or entering intensity and (back)scattered intensity. As shown in eqs. 4 & 5, it requires knowledge about the absorption coefficient, α, measured as described in section 4.2.

$$I_{scat} = -(1-\alpha) \cdot I_{rear} \qquad (4)$$

$$I_{rad} = I_{front} - I_{scat} \qquad (5)$$

The method which is presented here is based on separation of different sound field components via the spatial sound field information provided by an array. The radiated intensity is estimated as the intensity that would exist, if the incident (rear) and scattered field components could be taken away. So a free-field radiation condition is simulated. The idea is to first separate the incident field component into what is absorbed and what is scattered eq. (4), i.e. use separately measured information about the scattering/absorbing properties of the panel to calculate the scattered field, and finally subtract the incident and scattered fields from the total sound field. In this way the intensity is decomposed into separate components. Of special interest is the radiated (entering) intensity, which is the amount of sound energy that is entering into a cabin due to the external forces.

4.4 Panel contribution analysis, PCA

As a final consequence of being able to map the interior panels in a cabin with a long list of different sound field quantities, it is also desirable to calculate the contribution from the various panels to the perceived pressure at the operators/drivers position, see figure 7a. The idea was first presented in Ref. [12].

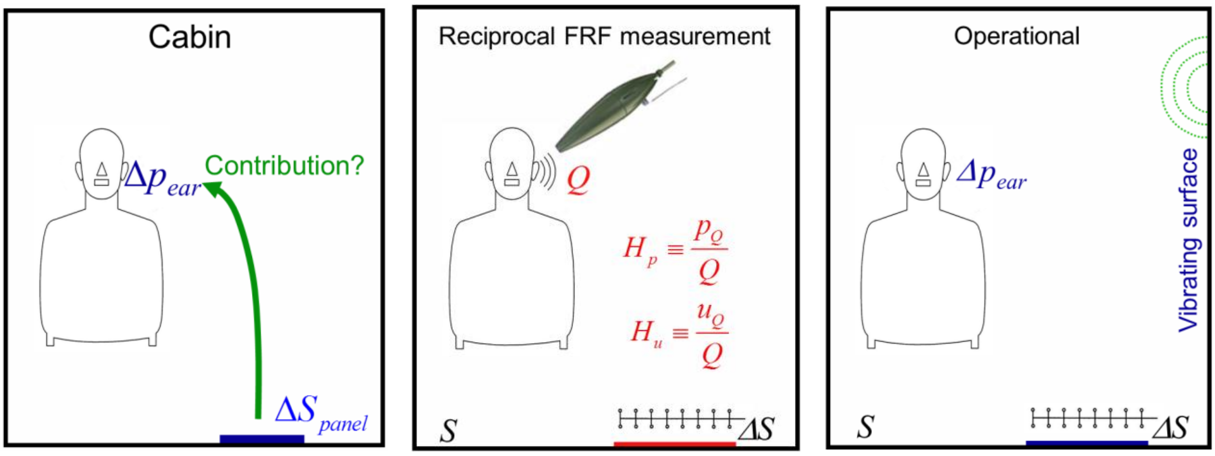

Figure 7a – Panel contribution analysis, PCA

Figure 7b – Reciprocal FRF measurements of PCA

Figure 7c – Operational measurements of PCA

The sound pressure contribution at a position in a cabin (figure 7a) from a section ΔS_{panel} can be expressed as:

$$\Delta p_{ear} = \iint_{\Delta S} [H_{p,Q}\, u_n - H_{u,Q}\, p] dS \tag{6}$$

where p is the sound pressure on the panel section, u_n is the particle velocity in the normal direction of the surface, and $H_{p,Q,}$ and $H_{u,Q}$ are the two frequency response functions (FRFs) from volume velocity to pressure and velocity on the panels (figure 7b).

The FRFs are measured by placing a volume velocity source (VVS) at the target position, e.g., the driver's ear position (figure 7b) and calculating the resulting sound pressure and particle velocity on the panels. This is done by measuring the sound pressure with a microphone array (DLA) at different positions covering the panels of interest, and then applying the ESM or SONAH algorithm to get pressure and velocity at the surface. Using the output from holography together with the measured radiated volume velocity from the VVS, the FRFs can be directly calculated.

Next, array measurements are performed under operational conditions (figure 7c), and the resulting surface quantities, p and u_n, are found by applying the ESM/SONAH algorithm again. ESM/SONAH requires a coherent field as input, but in the operational mode we may have several uncorrelated sources in the cabin. Here as well as in all other methods principal component decomposition (PCD) is used in order to decompose the sound field into a set of coherent subfields, which can be treated independently. The input to the PCD algorithm is cross-spectra between a set of reference signals and the signals from the array microphones and the cross-spectra between the reference signals. There should be at least as many references as there are uncorrelated sources.

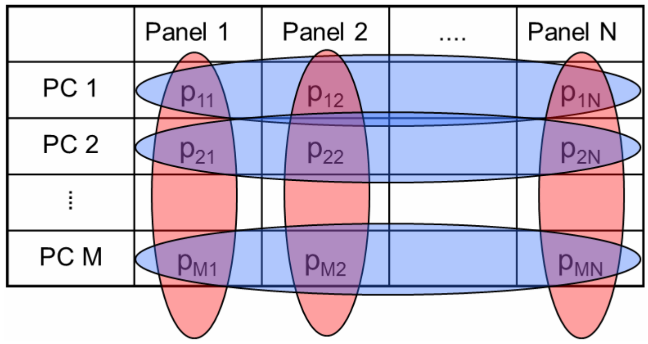

Figure 8 – For a specific principal component the panel contribution are added on vector basis (indicated by blue), while for a specific panel the contribution of the principal component, PC X are added on power basis (indicated by red)

Detailed example of a panel contribution analysis, PCA inside a car cabin is found in Ref. [13]. An example is shown in figure 9, where the five most dominating panels are indicated: wind shield, right side of dashboard, center console, right front floor and front roof, as well as the total (complex summation) is shown.

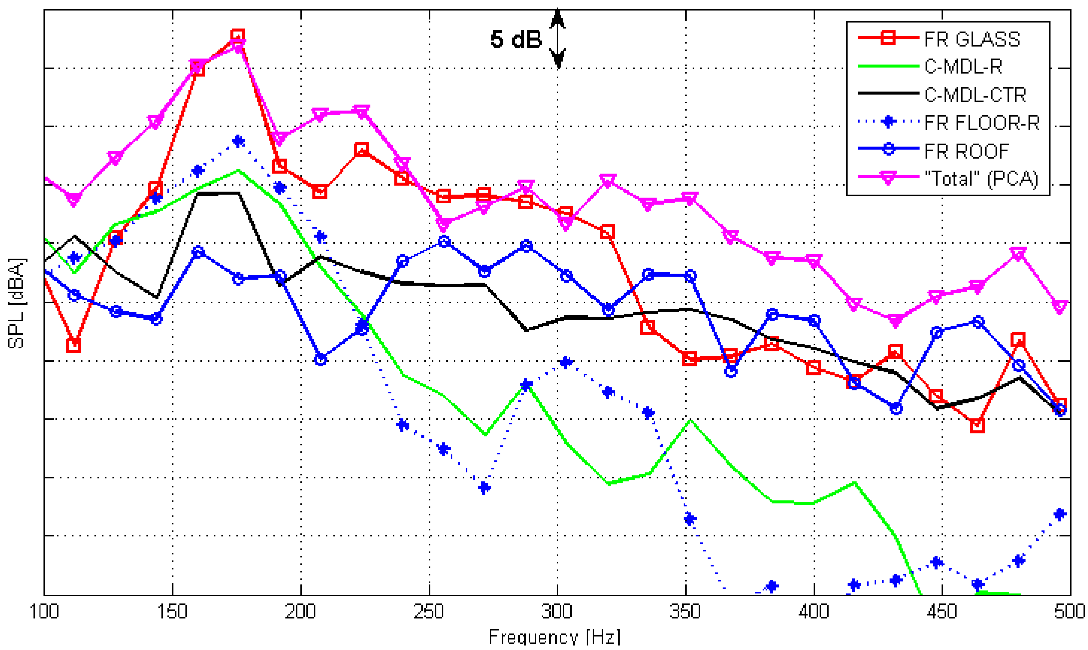

Figure 9 – Panel contribution analysis at driver's position inside a passenger vehicle. Below 325Hz the wind shield (red curve) is the dominating contributor. Above 325 Hz the front roof (blue curve) becomes a significant contributor at several frequencies

Actually complex panel contribution is calculated as indicated in figure 8. For each principal component (PC) the contribution are added on vector basis, i.e. the total contribution may be smaller than the contribution from the most dominating panel (e.g. around 175 Hz, 260 Hz & 300 Hz on figure 9). The contribution from the various principal components to a specific panel on the other hand is done on power (rms) basis since principal components are incoherent, i.e. there is no meaningful phase relationship between principal components.

5. SUMMARY/CONCLUSIONS

Figure 10 gives an overview of how to perform the measurement for the various four applications. Patch holography, absorption coefficient and basic intensity component analysis require only one type of measurements, while panel contribution and advanced intensity component analysis are combinations of two sets of measurement (one operational measurement and one "laboratory" measurement). The requirements for the additional measurements compared to performing basic patch holography are summarized in table 1.

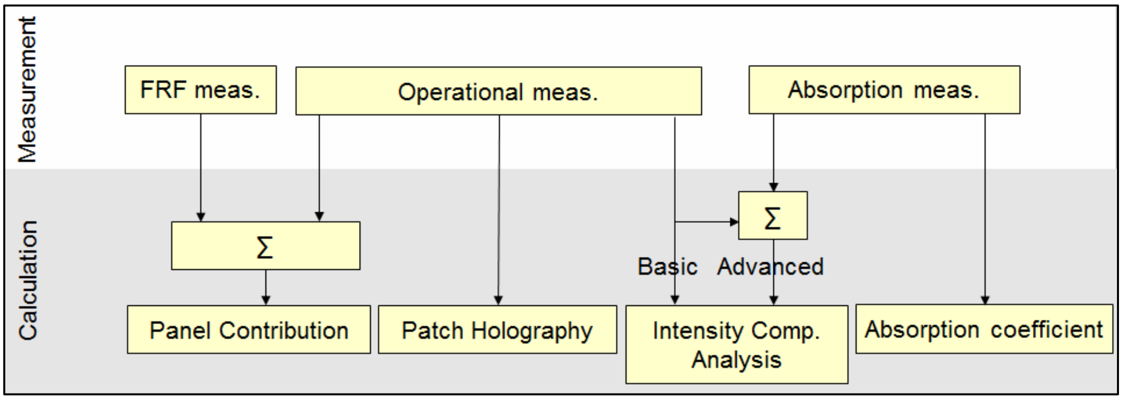

Figure 10 – Overview of the various measurement combinations for the four hand held array applications

Patch holography is performed by measuring close to the vibrating panels in order to map the noise radiation. Absorption measurements are done the same way except that the panels are absorbing sound, which has to be generated by loudspeakers.

Table 1 – Major properties of the three additional applications to patch holography. Advanced Intensity Component analysis (indicated in brackets) requires absorption measurements

	Absorption	**Intensity Component**	**Panel Contribution**
Output	α , $I_{total} \sim I_{net}$	I_{front} , I_{rear} I_{total} , ($I_{radiated}$, $I_{scattered}$)	PCA spectra, p-FRF, v-FRF, I, p, v
Extra Equipment	Exitation Sources		VVS Source, References
Measurement Type	Absorption	Operational, (Absorption)	Operational, FRF
Assumptions	Stationary sound field		
		(Local Reaction)	Decoupled Panels

Panel contribution (for example to the driver's ear position) requires measurements of frequency response functions (FRF) by use of a Volume Velocity Source from listening position (driver's ear) to the panels of interest in combination with measuring the patch holography patches in operational condition.

Figure 6a illustrates the basic three sound intensity components measured with a DLA. Figure 6b indicates how front intensity can be further decomposed into radiated (entering) and scattered components, if/when knowledge about the absorption coefficient is available.

Advanced intensity component analysis requires measurement of the absorption coefficient in combination with a patch holography measurement in operational condition. In this way the measured intensity can be decomposed into all its various components.

REFERENCES

[1] J.D. Maynard, E.G. Williams and Y. Lee: “Nearfield acoustic holography: I. Theory of generalized holography and the development of NAH”, (Journal Acoustical Society America 78(4), pp. 1395 – 1413, October 1985)

[2] Earl G. Williams: “Fourier Acoustics, Sound Radiation and Nearfield Acoustical Holography”, (Acedemic Press, London, Book 306pp. 1999)

[3] W.A. Veronesi and J.D. Maynard: “Nearfield acoustic holography (NAH) II. Holographic reconstruction algorithms and computer implementation”, (Journal Acoustical Society America 81(5), pp. 1307 – 1322, May 1987)

[4] J. Hald: “STSF – a unique technique for scan based Near-field Acoustic Holography without Restrictions on Coherence”, (Brüel & Kjær Technical Review no. 1, 1989)

[5] K.B. Ginn and J. Hald: “STSF – Practical instrumentation and applications”, (Brüel & Kjær Technical Review no. 2, 1989)

[6] R. Steiner and J. Hald: “Nearfield Acoustical Holography Without the Errors and Limitations Caused by the Use of Spatial DFT”, (International Journal of Acoustics and Vibration, 6 (2), June 2001)

[7] J. Hald, “Planar Near-field Acoustical Holography with Arrays Smaller Than the Sound Source”, Proceedings of ICA (2001)

[8] J. Hald: “Combining NAH and Beamforming Using the Same Array”, (Brüel & Kjær Technical Review no. 1, 2005)

[9] M. Pinho and J. Arruda: “On The Use of the Equivalent Source Method for Nearfield Acoustic Holography”, (ABCM Symposium Series in Mechatronics – Vol. 1- pp. 590-599, 2004)

[10] J. Gomes: “Patch holography using a double layer microphone array”, Proceedings of Inter-noise, (2007)

[11] J. Mørkholt, J. Hald and S. Gade: “Measurement of Absorption Coefficient, Radiated and Absorbed Intensity on the panels of a Vehicle Cabin using a Dual Layer Array with Integrated Position Measuremen”, JSAE Paper 20105022, (2010)

[12] J. Hald: “ Panel Contribution analysis using a Volume Velocity Source and a Double Layer Array with SONAH Algorithm”, Proceedings of Inter-noise, (2006)

[13] J. Gomes, M. Wada, Y. Fukuju, Y. Ishii, J. Hald, T. Satoh: “In-cabin Array-based Panel Contribution Analysis with a Vehicle Running on a Dyno”, JSAE Paper 20115359, (2011)

[14] J. Hald: “Performance Investigation of the Dual-Layer Array (DLA) at Low Frequencies”, (Brüel & Kjær Technical Review No. 1, 2011)

[15] J. Hald, J. Mørkholt, P. Hardy, D. Trentin, M. Bach-Andersen and G. Keith: “Array Based measurement of radiated and absorbed sound intensity components”, Proceedings of EuroNoise, (2008)